J Stat Phys (2008) 132: 707–719
DOI 10.1007/s10955-008-9585-0

Boundary Chromatic Polynomial

Jesper Lykke Jacobsen · Hubert Saleur

Received: 20 March 2008 / Accepted: 10 June 2008 / Published online: 25 June 2008

Abstract We consider proper colorings of planar graphs embedded in the annulus, such that vertices on one rim can take Q_{s} colors, while all remaining vertices can take Q colors. The corresponding chromatic polynomial is related to the partition function of a boundary loop model. Using results for the latter, the phase diagram of the coloring problem (with real Q and Q_{s}) is inferred, in the limits of two-dimensional or quasi one-dimensional infinite graphs. We find in particular that the special role played by Beraha numbers $Q = 4\cos^2\frac{\pi}{n}$ for the usual chromatic polynomial does not extend to the case $Q \neq Q_{\mathrm{s}}$. The agreement with (scarce) existing numerical results is perfect; further numerical checks are presented here.

Keywords Chromatic polynomial · Boundary loop model · Temperley-Lieb algebra · Graph colorings

1 Introduction

Let $G = (V, E)$ be a planar graph embedded in the annulus. Let $V_{\mathrm{s}} \subseteq V$ be the subset of vertices surrounding the face that contains the point at infinity. In other words, V_{s} are the vertices on the outer rim of the annulus. Place a spin variable $\sigma_i = 1, 2, \ldots, Q$ on each bulk vertex ($i \in V \setminus V_{\mathrm{s}}$) and a boundary spin $\sigma_j = 1, 2, \ldots, Q_{\mathrm{s}}$ on each boundary vertex ($j \in V_{\mathrm{s}}$). We suppose initially that $Q_{\mathrm{s}} \leq Q$, so that $Q - Q_{\mathrm{s}}$ of the colors allowed for the bulk spins are forbidden for the boundary spins.

J.L. Jacobsen (✉)
Laboratoire de Physique Théorique, École Normale Supérieure, 24 rue Lhomond,
75231 Paris Cedex 05, France
e-mail: jesper.jacobsen@ens.fr

J.L. Jacobsen · H. Saleur
Institut de Physique Théorique, CEA Saclay, 91191 Gif-sur-Yvette, France

H. Saleur
Department of Physics and Astronomy, University of Southern California, Los Angeles, CA 90089,
USA

The Potts model [1] partition function $Z_G(Q, Q_\mathrm{s}; \mathbf{v})$—also known to graph theorists as the multivariate Tutte polynomial [2]—can be defined through a slight generalization of the usual Fortuin-Kasteleyn expansion [3, 4]

$$Z_G(Q, Q_\mathrm{s}; \mathbf{v}) = \sum_{A \subseteq E} Q^{k(A)} \left(\frac{Q_s}{Q}\right)^{k_\mathrm{s}(A)} \prod_{e \in A} v_e \tag{1}$$

where $k(A)$ is the number of all connected components (clusters) in the graph induced by the edge subset A, and $k_\mathrm{s}(A)$ is the number of connected components that contain at least one vertex from V_s. In other words, Q_s (resp. Q) is the weight of a cluster that contains at least one (resp. does not contain any) vertex in V_s. The edge variables $\mathbf{v} = \{v_e\}_{e \in E}$ are related to the usual spin-spin couplings K_e through the relation $v_e = \exp(K_e) - 1$.

Note that in (1) there is no need for Q and Q_s to be integers, nor do we have to impose the constraint $Q_\mathrm{s} \leq Q$. We shall henceforth promote (1) to the *definition* of the (boundary) Potts model [5].

In this paper we wish to study the problem of proper colorings of G, such that bulk vertices can have Q different colors, whereas boundary vertices can have only a subset of Q_s colors. Adjacent vertices (of whatever type) are constrained to have different colors. The partition function $Z_G(Q, Q_\mathrm{s}; -1)$, i.e. with all $v_\mathrm{e} = -1$, counting the number of such proper colorings is referred to as the *boundary chromatic polynomial* and denoted $P_G(Q, Q_\mathrm{s})$. Note that $P_G(Q, Q)$ is nothing else than the usual chromatic polynomial, which has been studied extensively in the literature [6].

We address in particular the issue of the phase diagram of $P_G(Q, Q_\mathrm{s})$ for "large graphs"—what is meant precisely by this will be discussed below. The main result is the location and nature of a series of phase transition (with corresponding behaviors of zeroes of P_G) occurring when one varies one or both of the parameters Q and Q_s. We emphasize that most of our results are quite general, and do not depend on the detailed structure of the underlying graph G.

In the usual case $Q = Q_\mathrm{s}$, one of the striking features of the chromatic polynomial is that for "large graphs" its real zeroes possess accumulation points which belong to the magic set of Beraha numbers:[1]

$$B_t = 4\cos^2\left(\frac{\pi}{t}\right) \quad \text{for } t = 2, 3, \ldots. \tag{2}$$

Note that the first two such numbers are $Q = 0$ and $Q = 1$, which are usually exact zeroes for finite graphs as well. One of the striking conclusions of our study is that the special role played by Beraha numbers is not very resistant to changing Q_s. Depending on the problem one choses, there can indeed be accumulating zeroes at other special points of the real axis.

It is important to realize that the definition of $P_G(Q, Q_\mathrm{s})$, albeit very natural, can lead to counterintuitive features in particular when interpreted outside the initial domain of definition $Q_\mathrm{s} \leq Q$. For instance it turns out that for most graphs, $P_G(Q, Q_\mathrm{s})$ does not vanish when $Q = 0$ or $Q = 1$, even though in that case there is no way—forgetting the boundary contribution—to color the bulk vertices with Q colors. The point is that in the original definition (1), spins belonging to clusters that touch the boundary receive a fugacity Q_s,

[1] When $Q = Q_\mathrm{s}$, and for certain particular (non annular) choices of boundary conditions (see Sect. 7.2 of [7]), one also finds isolated real accumulation points which are *not* Beraha numbers. The existence of such points may presumably be traced back to accidental (non generic) degeneracies of eigenvalues in the transfer matrix spectra.

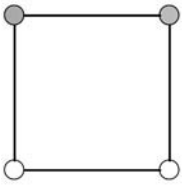

Fig. 1 For this graph (with the *shaded vertices* on the boundary) the chromatic polynomial continued from the region $Q \geq Q_s$ is $P_G = (Q^2 - 3Q + 3)Q_s(Q_s - 1)$. It does not vanish for $Q = 0$ nor $Q = 1$. Meanwhile the chromatic polynomial continued from the region $Q \leq Q_s$ is obtained—in this simple example—by exchanging Q and Q_s in the above expression, and does vanish for $Q = 0$ and $Q = 1$

which initially is assumed smaller or equal to Q, but which, after continuation, can in fact be greater, hence "pumping" the number of colors in the bulk. Figure 1 provides a simple example of this subtlety.[2]

One could define another chromatic polynomial starting from the situation where $Q \leq Q_s$. In terms of the subsequent cluster and loop model expansions, it would however be much less interesting. Indeed, in such a model, only clusters not containing any of the bulk spins would get the fugacity Q_s, and thus only loops "glued to the boundary" would get a fugacity different from the bulk ones. This presumably would not affect the patterns of zeroes.

The layout of the paper is as follows. In Sect. 2 we relate the boundary chromatic polynomial to a loop model which was previously introduced in [5] and further studied in [8]. In Sect. 3 the issue of the phase diagram is transposed into the setting of the Beraha-Kahane Weiss theorem [10] which we review. The necessary input for applying that theorem is supplied by an analytic continuation of the field theoretic results of [5], as explained in Sect. 4. Here we also arrive at the main results of the paper, which are the phase transition loci (15)–(16). All of this applies to the two-dimensional thermodynamic limit. However, the main results remain valid for quasi one-dimensional graphs, and we provide the necessary arguments in Sect. 5. A few numerical validations of our results are given in Sect. 6 after which we present our conclusions.

2 Boundary Loop Model

The cluster model (1) can obviously be defined for any graph G. However, when G is planar, the cluster model can be turned into a loop model on the medial graph $\mathcal{M}$.

We recall that the medial (or surrounding) graph has a vertex standing on each edge $e \in E$, and an edge between vertices standing on edges e_1, e_2, whenever e_1, e_2 are incident to a common vertex in V and surround a common face in G.

A non-intersecting transition system on $\mathcal{M}$ is defined locally as in Fig. 2. Globally, this transition system is a set of loops—or cycles in the standard graph theoretical terminology—which separate clusters in G from their duals. By the existence of a point at infinity, the

[2] To keep this example as elementary as possible, we deviate slightly from the above definition of V_s. In particular, Fig. 1 is not considered to be embedded in the annulus, nor does V_s consist of *all* the vertices surrounding the outer face. Clearly, the expansion (1)—and the discussion of the subtleties brought about by the initial $Q_s \leq Q$ constraint—apply to any graph G (planar or not), and for V_s any subset of V. However, the role of the Beraha numbers and the transformation to a (boundary) loop model are very particular to the planar case.

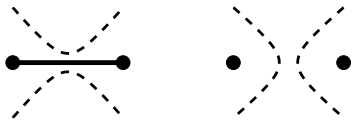

Fig. 2 The transition system (shown as *dashed lines*) depends on whether a given edge e (show as a *solid line*) is present in (*left panel*) or absent from (*right panel*) the edge subset $A \subseteq E$ in (3)

inside and outside of a loop are well defined. A loop that contains at least one vertex of V_s on its inside is called a boundary loop. A loop that is not a boundary loop is called a bulk loop.

Let now $\ell(A)$ be the total number of loops, and $\ell_\mathrm{s}(A)$ the number of boundary loops. By the Euler relation, one has $k(A) = \frac{1}{2}(\ell(A) + |V| - |A|)$, so that

$$Z_G(Q, Q_\mathrm{s}; \mathbf{v}) = Q^{|V|/2} \sum_{A \subseteq E} Q^{\ell(A)/2} \left(\frac{Q_\mathrm{s}}{Q}\right)^{\ell_\mathrm{s}(A)} \prod_{e \in A} x_e \tag{3}$$

where we have introduced $x_e = Q^{-1/2} v_e$. In other words, the weight of a bulk loop (resp. a boundary loop) is n (resp. n_s), subject to the relations

$$Q = n^2, \qquad Q_\mathrm{s} = n n_\mathrm{s}. \tag{4}$$

The boundary loop model (3) was introduced in [5], and further studied in a more general setting in [8]. The emphasis in [5, 8] was on the ferromagnetic case where all $x_e = 1$. We shall see now that the generalization of these results to the antiferromagnetic region (with $x_e < 0$) allows to infer the phase diagram of the boundary chromatic polynomial.

3 Beraha-Kahane-Weiss Theorem

We wish to study the boundary chromatic polynomial in the thermodynamic limit where G becomes large ($|V| \to \infty$). In general, one may take the limit $|V| \to \infty$ through a recursive family of graphs G_N embedded in the annulus, of width W and circumference N, such that $|V| \sim NW$ and $|V_\mathrm{s}| \sim N$. In particular one may think of strips of regular lattices (square, triangular, ...), but we emphasize that most of our results do not depend on the detailed structure of the graph, nor do they require that it be regular.

In Sect. 4 we take the width $W \propto N$, so that the limiting graph G_∞ is two-dimensional, and the results [5] of conformal field theory (CFT) apply. In Sect. 5, we consider instead W finite, so that G_∞ is quasi one-dimensional, and we shall see that the main results hold true in that case as well.

In both cases one may think of the partition function $P_G(Q, Q_\mathrm{s})$ as being built up by a transfer matrix, with time slices containing W spins. The structure of the transfer matrix has been discussed in details in [5], and in particular it was shown that each of its eigenvalues λ_i contributes to the partition function with a non-trivial multiplicity D_i that we shall refer to as an *eigenvalue amplitude*. Hence,

$$P_G(Q, Q_\mathrm{s}) = \sum_i D_i (\lambda_i)^N. \tag{5}$$

The fact that $D_i \neq 1$ in general can be traced back to the non-local nature of the loops defining (3), and to the periodic boundary conditions in the time direction.

We wish to study the phase diagram of the boundary chromatic polynomial by locating the accumulation points $\mathcal{A}$ of the partition function zeroes $P_G(Q, Q_s) = 0$ in the limit $N \to \infty$. Following Lee and Yang [9], this can be done by fixing one of the variables Q or Q_s (or by imposing a fixed relation among Q and Q_s), and letting the remaining variable (henceforth denoted z) take complex values.

Due to the form (5) the Beraha-Kahane-Weiss (BKW) theorem [10] applies. Let us call an eigenvalue λ_i dominant at z if $|\lambda_i(z)| \geq |\lambda_k(z)|$ for all k. The BKW theorem then states that (under very mild assumptions)

- $z \in \mathcal{A}$ is an isolated accumulation point iff there is a *unique* dominant eigenvalue λ_i at z and the corresponding amplitude vanishes, $\alpha_i(z) = 0$.
- $z \in \mathcal{A}$ forms part of a continuous curve of accumulation points iff there are *at least two* dominant eigenvalues at z. (In other words, z is the locus of a level crossing involving a dominant eigenvalue.)

It is not in general clear to what extent CFT predictions apply to complex values of the parameters Q and Q_s. But at least we can infer important information about the phase diagram by combining the BKW theorem [10] with the CFT results [5] for the special case of real parameter values.

4 Phase Diagram in the Thermodynamic Limit

It is useful to parametrize the bulk and boundary loop weights as follows

$$n = 2\cos(\pi e_0), \qquad n_s = \frac{\sin((r+1)\pi e_0)}{\sin(r\pi e_0)} \tag{6}$$

defining the parameters e_0 and $r \in (0, \frac{1}{e_0})$. The continuum theory then has central charge

$$c = 1 - \frac{6e_0^2}{1 - e_0}. \tag{7}$$

The range $e_0 \in [0, \frac{1}{2})$ describes the usual ferromagnetic-paramagnetic transition, corresponding to positive values of n and n_s.

We here need the analytic continuation into the range $e_0 \in (\frac{1}{2}, 1)$, where n and n_s become negative. This range was referred to as the Berker-Kadanoff (BK) phase in [11, 12]. Inspecting Fig. 2 it is easy to see that (3) is invariant under a simultaneous sign change of n, n_s, and x_e. The BK phase therefore corresponds to negative values of x_e, i.e., it describes a part of the antiferromagnetic region of the Potts model. Its relevance to the chromatic line $v_e = -1$ is due to the fact that the temperature variable v_e is an *irrelevant* perturbation in the BK phase, in the sense of the renormalization group. The BK phase therefore controls, for any fixed $Q \in (0, 4)$, a *finite* range of values v_e. One may therefore expect that at least for $Q < Q_c$, where $Q_c \leq 4$ is some lattice-dependent constant, the BK phase will control the chromatic line $v_e = -1$.

To give a little more substance to this general discussion, it is worthwhile to recall some exact information about the special cases of the square and triangular lattices. The standard

Potts model ($Q_s = Q$ and $v_e = v$) is then exactly solvable on the curves [13, 14]

$$\begin{aligned} v^2 &= Q \quad \text{(square lattice)}, \\ v^3 + 3v^2 &= Q \quad \text{(triangular lattice)}. \end{aligned} \tag{8}$$

In view of the parametrization (6) it is more convenient to rewrite this as

$$\begin{aligned} v &= 2\cos(\pi e_0) \quad \text{(square lattice)}, \\ v &= -1 + 2\cos\left(\frac{2\pi e_0}{3}\right) \quad \text{(triangular lattice)} \end{aligned} \tag{9}$$

where $e_0 \in [0, 1]$ for the square lattice and $e_0 \in [0, \frac{3}{2}]$ for the triangular lattice.

Both analytical and numerical studies of the Potts model with $Q_s = Q$ and either free or periodic transverse boundary conditions conclude that the critical exponents along the curves (8) for $e_0 \in [0, 1)$ are those predicted by the CFT. In particular, the central charge is (7) as claimed. Moreover, the exponents for $e_0 \in (\frac{1}{2}, 1)$ are just the analytic continuations of those valid for the usual ferromagnetic regime $e_0 \in (0, \frac{1}{2})$. This already strongly suggests that the critical properties for $e_0 \in [0, 1)$ are lattice-independent (universal).[3] This conclusion is further corroborated by the so-called Coulomb gas approach [15] to CFT.

Further studies have established that for each $Q \in (0, Q_c)$ the chromatic polynomial indeed renormalizes to the BK phase, with the following values of Q_c for the square [17] and triangular [18–20] lattices

$$\begin{aligned} Q_c &= 3 \quad \text{(square lattice)}, \\ Q_c &= 3.8196717312\ldots \quad \text{(triangular lattice)}. \end{aligned} \tag{10}$$

We now return to the main objective of this section, which is to establish the critical behavior of the boundary chromatic polynomial. On general grounds, boundary conditions should not modify bulk RG flows.[4] Therefore, we expect the analytic continuation of the CFT results [5] to the range $e_0 \in (\frac{1}{2}, 1)$ to describe the critical behavior of the boundary chromatic polynomial for $Q \in (0, Q_c)$.

It is convenient to set $e_0 = 1 - \frac{1}{t}$, so that the BK phase corresponds to $t > 2$. The parameter r appearing in (6) is then constrained to $r \in (0, \frac{t}{t-1})$. We have

$$\begin{aligned} n &= -2\cos\left(\frac{\pi}{t}\right), \\ n_s &= -\frac{\sin(\frac{(r(t-1)-1)\pi}{t})}{\sin(\frac{r(t-1)\pi}{t})}. \end{aligned} \tag{11}$$

[3] In the case of the triangular lattice, the range $e_0 \in (1, \frac{3}{2}]$ describes a very different CFT [16] which we shall not need further in the present work.

[4] This is of course a subtle issue in cases such as this one, where the statistical models are not very physical. In fact, there *are* some boundary terms that can profoundly affect the behavior of flows in the Berker-Kadanoff phase—for instance those breaking the quantum group symmetry in the XXZ chain version of the models. For the boundary terms we are considering however—which can be described through the boundary Temperley Lieb algebra—no such "rogue" behavior seems to occur.

In this parametrization, $Q = n^2$ (see (4)) is nothing else than the tth Beraha number B_t defined in (2). Real chromatic zeroes have long been known [6] to accumulate around B_t for integer values of $t \geq 2$. One major motivation of this work is to show that the special role played by the Beraha numbers is destroyed by choosing $Q_s \neq Q$.

As explained in [5] the detailed transfer matrix structure implies that each eigenvalue appearing in (5) is in fact an eigenvalue of a modified transfer matrix in which the number of loops winding around the periodic direction of the annulus (i.e., which are non-homotopic to a point) is fixed. Each eigenvalue can thus be labelled by the corresponding number of winding loops $L = 0, 2, 4, \ldots$, as $\lambda_i^{(L)}$. By the definition of the Potts model and the medial graph $\mathcal{M}$, the corresponding number of winding clusters is $L/2$. In each sector with $L > 0$, the dominant eigenvalue corresponds to the outermost of the winding loops being constrained to be a boundary loop (i.e., we can restrict to what was called the "blobbed sector" in [5, 8]).

The existence of L winding loops corresponds in CFT to the insertion of a pair of so-called L-leg operators $\mathcal{O}_L$ at the extremities of the strip; the extremities are subsequently glued together to form the annulus with periodic boundary conditions in the time direction. The asymptotic scaling for $W \gg 1$ of the dominant eigenvalue $\lambda_0^{(L)}$ in each sector L is then fixed by CFT as [21]

$$\frac{\lambda_0^{(L)}}{\lambda_0^{(0)}} = \exp\left(-\frac{\pi h_L}{W}\right) + \cdots \tag{12}$$

where the dots on the right-hand side represent terms that decay faster than $\exp(-\text{const}/W)$.

The constant h_L appearing in (12) is the so-called conformal weight of the L-leg operator (in the "blobbed sector") whose value has been established in [5, 22]. After the analytic continuation implied by the parametrization (11), this reads

$$h_L = \frac{1}{4t}\left(L^2 - 2rL(t-1) + (r^2-1)(t-1)^2\right). \tag{13}$$

The corresponding eigenvalue amplitude has been derived rigorously in [5]:

$$D_L = \begin{cases} 1 & \text{for } L = 0, \\ n_s U_{L-1}(n/2) - U_{L-2}(n/2) & \text{for } L > 0 \end{cases} \tag{14}$$

where $U_j(x)$ is the jth order Chebyshev polynomial of the second kind.

Note that in the probabilistic regime ($e_0 \in [0, \frac{1}{2}]$) the continuum limit is dominated by $L = 0$. This is no longer true in the BK phase, where for any t there is at least one of the exponents h_L taking negative values. The most negative exponent determines the most "probable" number of winding loops. This situation is clearly counter-intuitive from a probabilistic point of view, but it is made possible by the appearance of negative Boltzmann weights. Note also that the invariance of (3) under a simultaneous sign change of n, n_s, and x_e is not sufficient to make all weights positive.

Using (12), dominant level crossings of transfer matrix eigenvalues correspond asymptotically (for $W \gg 1$) to level crossings of the conformal weights h_L. We can thus read directly from (13) the necessary and sufficient criterion for the second part of the BKW

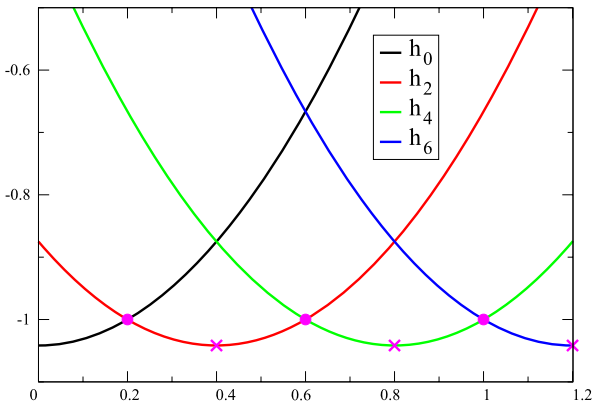

Fig. 3 Conformal weights h_L as functions of the parameter r for the case $t = 6$. Dominant level crossings and vanishing dominant amplitudes are shown respectively as *solid circles* and *crosses*

theorem. Indeed, level crossings involving the dominant L-leg sector occur when

$$h_L = h_{L+2} \quad \Longleftrightarrow \quad r = \frac{L+1}{t-1} \tag{15}$$

with $L \leq t-1$. In particular, h_L is the most negative exponent for $r \in (\frac{L-1}{t-1}, \frac{L+1}{t-1})$.

Similarly, the necessary and sufficient criterion for the first part of the BKW theorem is read off from (14). Indeed, the amplitude of the dominant L-leg sector vanishes when

$$D_L = 0 \quad \Longleftrightarrow \quad r = \frac{L}{t-1} \tag{16}$$

with $L = 2, 4, 6, \ldots$.

These phenomena are illustrated in Fig. 3 for the case $t = 6$ (the $Q = 3$ state Potts model).

For any fixed n, phase transitions will therefore take place for $r = s/(t-1)$ and integer $s \in (0, t]$. The corresponding value of the boundary parameter is

$$n_{\mathrm{s}} = -\frac{\sin(\frac{(s-1)\pi}{t})}{\sin(\frac{s\pi}{t})}. \tag{17}$$

For even s this corresponds to a vanishing dominant amplitude, and for odd s to a dominant level crossing. The corresponding value of the dominant exponent (13) is $h_L = -\frac{(t-1)^2}{4t}$ for any even s, and $h_{\mathrm{L}} = \frac{2-t}{4}$ for any odd s.

The $N \to \infty$ limiting curve of accumulation points of partition function zeroes in the complex Q_{s} plane (in the vicinity of the real Q_{s} axis) can now be inferred from the BKW theorem: For even s one has an isolated real accumulation point, and for odd s a continuous curve of accumulation points intersects the real axis.

In the example $t = 6$ of Fig. 3, the transitions at $r = \frac{1}{5}, \frac{2}{5}, \frac{3}{5}, \frac{4}{5}, 1, \frac{6}{5}$ correspond to the following numbers of boundary colors: $Q_{\mathrm{s}} = 0, 1, \frac{3}{2}, 2, 3, \infty$.

The discussion following (16) has subsumed that we are interested in the phase diagram for fixed Q and varying Q_{s}. But of course the criteria (15)–(16) for phase transitions hold true for other situations as well. In particular, the following few useful cases correspond to

simple relations between r and t:

$$\begin{aligned}
Q_{\rm s} &= Q && : \quad r = 1, \\
Q_{\rm s} &= Q-1 && : \quad r = (t-2)/(t-1), \\
Q_{\rm s} &= Q-2 && : \quad r = (t-2)/(2t-2), \\
Q_{\rm s} &= Q-\sqrt{Q} && : \quad r = 1/2, \\
Q_{\rm s} &= 0 && : \quad r = 1/(t-1), \\
Q_{\rm s} &= 1 && : \quad r = 2/(t-1), \\
Q_{\rm s} &= 2 && : \quad r = (t+2)/(2t-2), \\
Q_{\rm s} &= \tfrac{1}{2}Q && : \quad r = t/(2t-2).
\end{aligned} \tag{18}$$

For all of these, (15)–(16) yield phase transitions located at *integer* values of t (i.e., at the Beraha numbers B_t), but this needs of course not be the case for more general choices of $Q_{\rm s}$.

5 Quasi One-Dimensional Case

We now turn to the quasi one-dimensional geometry where the circumference of the annulus $N \to \infty$, while is width W is kept fixed and finite. In that case, the possible number of winding loops is constrained by $L \leq 2W$.

Equation (14) for the eigenvalue amplitudes was in fact derived combinatorially for finite W, and so remains valid in this case. On the other hand, (13) must be discarded, since its derivation supposed the validity of conformal field theory. However, the pleasant surprise is that even for finite W the dominant eigenvalues in the L and $(L+2)$ leg sectors cross exactly for the values of r and t given by (15).

This coincidence follows from representation theory of the underlying boundary Temperley-Lieb algebra. While this algebra is semi-simple for generic values of the parameters, it admits families of degeneracy points where generically irreducible representations merge into larger indecomposable representations. Results in [23] guarantee that this occurs for finite values of W exactly at the same values that lead to the coincidences (15) of the conformal weights in the continuum limit. To be a little more explicit, let us use again the parametrization (6) so that the γ in [23] is πe_0. Then when $r = \frac{L+1}{t-1}$ as in (15) we can rewrite $n_{\rm s} = \frac{\sin L\gamma}{\sin(L+1)\gamma}$ so we are in a degenerate case (19) of [23] with $\eta = (L+1)\gamma$ there. The embedding (16) of [23] with $n_c = L+1$ and $l = 1$ guarantees the coincidence (15).

When $r = 1$—in the original parametrization (6)—this can be understood somewhat more easily by using quantum group representation theory [24], as the generic $U_q(sl(2))$ representations for sectors L and $L+2$, of spin $j = L/2$ and $j = L/2+1$, merge into larger indecomposable representations. When r is integer larger than one, this can be explained similarly by the construction of Sect. 5 in [5]. Indeed, there the effect of the boundary weight $n_{\rm s}$ was obtained algebraically by adding r extra strands on the outside of the annulus, subject to the action of a certain symmetrizer. Thus, the boundary loop model (3) with r integer is a special case of the standard loop model in which only the weight n appears. The latter is known to have an $U_q(sl(2))$ quantum group symmetry [24], and this in fact implies that (15) still holds true. The presence of exact coincidences at arbitrary r can maybe be interpreted in terms of some quantum group—the commutant of the boundary Temperley-Lieb algebra—but we will not discuss this here.

The key results of Sect. 4 therefore remain valid, up to two subtle effects to be discussed below.

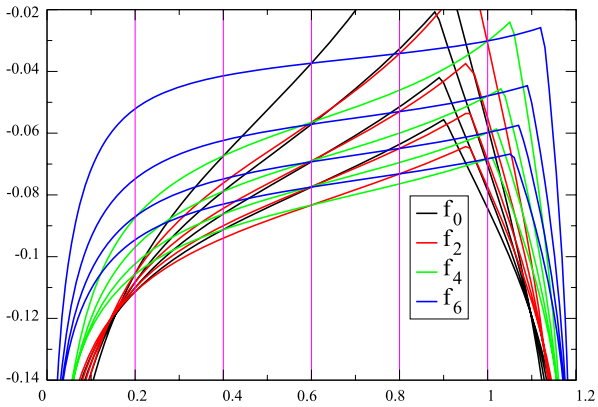

Fig. 4 Leading free energies f_L in the sectors $L = 0, 2, 4, 6$ as functions of $r \in (0, \frac{6}{5})$. The boundary loop model is here defined on the square lattice, along the BK critical curve, and the parameter $t = 6$. Four different system sizes ($W = 8, 10, 12, 14$) are shown, the largest size corresponding to the lowermost curves. The *vertical lines* are guides to the eye

To make this conclusion more accessible to readers unacquainted with quantum groups we turn to a numerical verification. Figure 4 shows the leading free energies $f_L = -\frac{1}{W}\log\lambda_0^{(L)}$ in the L-leg sector, as functions of r in the parametrization (11), for four different values of W. The results were obtained for the square lattice in the diagonal geometry defined in [5], along the curve (9) with $e_0 \in (\frac{1}{2}, 1)$, i.e., within the BK phase. Results for other lattices would be similar, provided that one remains inside the domain of attraction of the BK phase.

For each W, the dominant level crossings are seen to occur exactly as predicted by (15). More generally, the r values singled out by (15)–(16) are seen to be the loci of subdominant level crossings as well, as would be expected from an underlying quantum group symmetry.

Figure 4 was made for the choice $t = 6$ (the $Q = 3$ state Potts model), so that it is the precise finite-size analogue of Fig. 3. Other, non-integer choices of t were found to lead to the same conclusions.

We still need to discuss the two subtle effects referred to above. The first one is that if the annulus is too narrow ($2W < \lfloor t \rfloor$) to accomodate the number of legs required by dominant sector with the largest L predicted by (15), the corresponding level crossings will simply be absent, and the $2W$-leg sector will remain dominant for the corresponding values of the parameter r.

The second effect is that Fig. 4 gives clear evidence that when r becomes too large, there is an internal level crossing in each L-leg sector, visible as a cusp in the curves. To the right of these cusps the pattern of dominance may change. A detailed analysis of the loci of the cusps reveals that their position tends to $r = 1$ as $W \to \infty$, independently of the value of L. Moreover, for $r \in (1, \frac{t}{t-1})$ it is the $L = 0$ sector that will be dominant for large enough W.

6 Numerical Verifications

To conclude this paper, we wish to check that the predictions of Sects. 4–5 agree with existing numerical results on the limiting curves $\mathcal{A}$ of chromatic zeroes. The goal of this comparison is furthermore to convince the reader that our results are:

1. Lattice independent;
2. Independent of v_e, as long as we are in the BK phase;
3. Correct for various choices of Q_s.

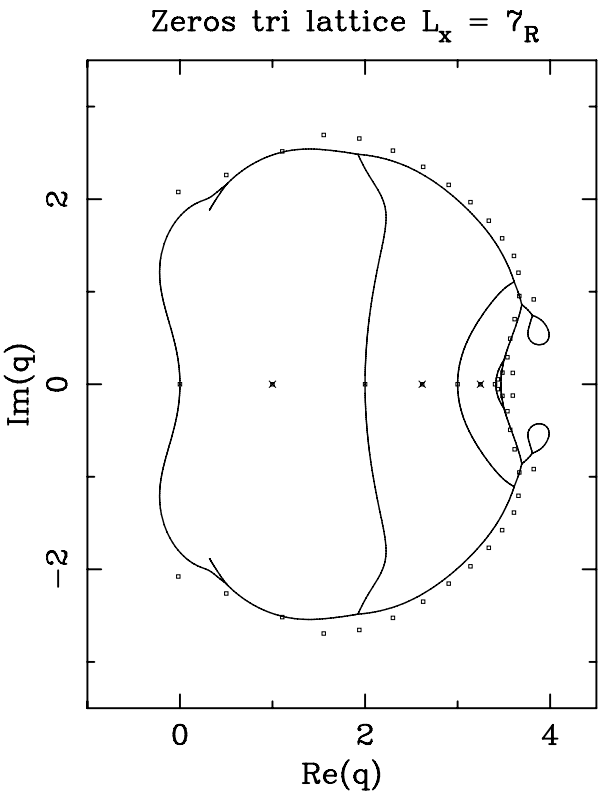

Fig. 5 Zeroes in the complex Q plane of the triangular-lattice chromatic polynomial on an $W \times N$ annulus for $W = 7$ and $N = 35$, and their accumulation points as $N \to \infty$. The boundary parameter $Q_s = Q$. Taken from Fig. 7 of [25]

Figure 5 shows the accumulation points $\mathcal{A}$ for the triangular-lattice chromatic polynomial on an annulus of width $W = 7$. Transverse boundary conditions are free, so that $Q_s = Q$. The agreement with the predictions (15)–(16) for the real accumulation points is perfect. There is one additional real accumulation point at $Q_c(W) = 3.4682618071\ldots$ which is a finite-size analogue of Q_c discussed in Sect. 4. As $W \to \infty$ we expect $Q_c(W) \to Q_c$ given by (10).

Figure 6 shows the accumulation points $\mathcal{A}$ of partition function zeroes for a square-lattice Potts model along the curve (8). The geometry is that of an annulus of width $W = 3$ with free transverse boundary conditions. However, all vertices on the outer rim of the annulus are connected to an extra exterior vertex. Therefore, the vertices on the outer rim (call them V_s) support spins which are effectively constrained to take only $Q_s = Q - 1$ different values (since they must be different from the value of the exterior spin). The partition function on the graph just described is therefore equal to $QZ_G(Q, Q_s = Q - 1; v_e = \pm\sqrt{Q})$ in our notation, where now G is just an ordinary annulus of width W, with no extra exterior vertex.

Once again, the agreement with the predictions (15)–(16) for the real accumulation points is perfect. In particular, it follows easily from the predictions that the loci of isolated real accumulation points and curves of accumulation points intersecting the real Q-axis are swapped between Figs. 5 and 6. Along the curve (8) we would expect the BK phase to terminate only at $Q_c = 4$. Thus, the phase transition corresponding to the largest possible L-sector becoming dominant is limited by the available width as $L \leq 2W$. This is again in perfect agreement with Fig. 6. Similar agreements are found with the numerical results for

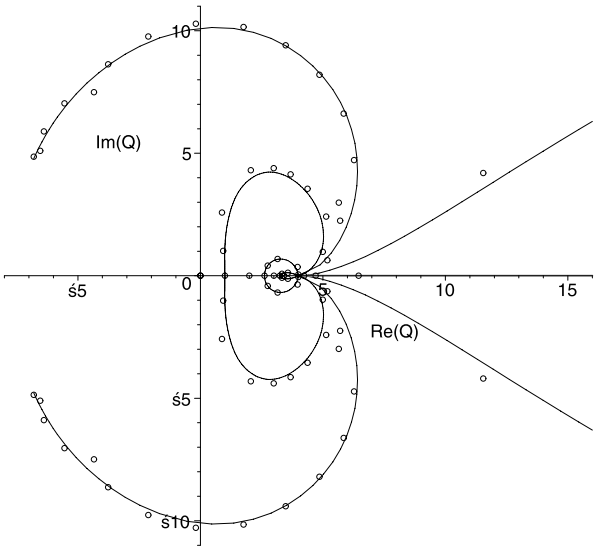

Fig. 6 Zeroes in the complex Q plane of a square-lattice Potts model along the curve (8) on an $W \times N$ annulus for $W = 3$ and $N = 26$, and their accumulation points as $N \to \infty$. The boundary parameter $Q_s = Q - 1$. Taken from Fig. 5 of [26]

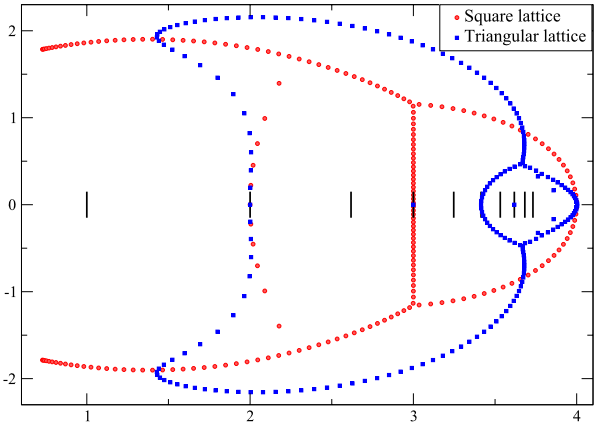

Fig. 7 Zeroes in the complex Q plane of the $Q_s = Q - 2$ boundary chromatic polynomials on an $W \times N$ annulus, with $W = 2$ and $N = 100$, for both the square and the triangular lattice. The *black vertical lines* indicate the positions of the Beraha numbers (2)

real accumulation points given in [26] in the case $W = 4$ (for which the complete limiting curve $\mathcal{A}$ was not computed).

As a final check, we have computed the boundary chromatic polynomials with $Q_s = Q - 2$ on an $W \times N$ annulus for $W = 2$ and $N = 100$, for both the square and the triangular lattice. Their zeroes in the complex Q plane are shown in Fig. 7. The agreement between (15)–(16) and the real accumulation points for the triangular lattice is striking. Notice in particular that we predict in general that only Beraha numbers of even order, viz. B_t with $t = 4, 6, 8, 10, \ldots$, can appear as accumulation points on the real Q axis. For the square lattice, the branch cutting the real axis at $Q = 3$ marks the termination of the BK phase, in agreement with (10); to the right of this branch one does not observe any further structure as expected.

7 Conclusion

To summarize, we have introduced a new graph coloring problem—the boundary chromatic polynomial—and identified the loci of phase transitions for real values of the parameters Q and Q_s. Our results are lattice independent, and valid not only on the chromatic line but in the entire Berker-Kadanoff phase.

While we have provided a number of striking numerical tests that validate our analytical predictions, we believe we have left ample space for further numerical investigations of the boundary chromatic zeroes for families of graphs embedded in the annulus.

A straightforward extension of the work presented here would be to consider graphs on an annulus for which bulk spins can take values $1, 2, \ldots, Q$, whereas spins on the outer (resp. inner) rim of the annulus are constrained to take values $1, 2, \ldots, Q_o$ (resp. $1, 2, \ldots, Q_i$). Note that in the cluster expansion analogous to (1), the number of spin values accessible to clusters touching both rims can be taken as a further independent variable Q_b, not necessarily equal to $\min(Q_o, Q_i)$.

Recent work on the corresponding two-boundary loop model furnishes the results for the eigenvalue amplitudes [8] and the critical exponents [27], analogous to (13)–(14) of this article. The phase diagram for real parameter values Q, Q_o, Q_i, Q_b can therefore be worked out along the lines presented here.

Acknowledgements We thank the authors of [25, 26] for the permission to reproduce Figs. 5–6. This work was supported by the European Community Network ENRAGE (grant MRTN-CT-2004-005616), by the Agence Nationale de la Recherche (grant ANR-06-BLAN-0124-03), and by the European Science Foundation network program INSTANS. One of us (JLJ) further thanks the Isaac Newton Institute for Mathematical Sciences, where part of this work was done, for hospitality.

References

1. Wu, F.Y.: Rev. Mod. Phys. **54**, 235–268 (1982). Erratum: Wu, F.Y.: Rev. Mod. Phys. **55**, 315 (1983)
2. Sokal, A.D.: In: Bridget, S. (ed.) Surveys in Combinatorics 2005, pp. 173–226. Cambridge University Press, Cambridge (2005). math.CO/0503607
3. Kasteleyn, P.W., Fortuin, C.M.: J. Phys. Soc. Jpn. Suppl. **26**, 11 (1969)
4. Fortuin, C.M., Kasteleyn, P.W.: Physica **57**, 536 (1972)
5. Jacobsen, J.L., Saleur, H.: Nucl. Phys. B **788**, 137–166 (2008). math-ph/0611078
6. Salas, J., Sokal, A.: J. Stat. Phys. **104**, 609–699 (2001). cond-mat/0004330
7. Jacobsen, J.L., Salas, J., Sokal, A.: J. Stat. Phys. **112**, 921–1017 (2003). cond-mat/0204587
8. Jacobsen, J.L., Saleur, H.: J. Stat. Mech. Theory Exp. P01021 (2008). arXiv:0709.0812
9. Yang, C.N., Lee, T.D.: Phys. Rev. **87**, 404 (1952)
10. Beraha, S., Kahane, J., Weiss, N.J.: Proc. Nat. Acad. Sci. USA **72**, 4209 (1975)
11. Saleur, H.: Commun. Math. Phys. **132**, 657 (1990)
12. Saleur, H.: Nucl. Phys. B **360**, 219 (1991)
13. Baxter, R.J.: J. Phys. C **6**, L445–L448 (1973)
14. Baxter, R.J., Temperley, H.N.V., Ashley, S.E.: Proc. R. Soc. Lond. A **358**, 535–559 (1978)
15. Nienhuis, B.: In: Domb, C., Lebowitz, J.L. (eds.) Phase Transitions and Critical Phenomena, vol. 11. Academic, London (1987)
16. Jacobsen, J.L., Saleur, H.: Nucl. Phys. B **743**, 207–248 (2006). cond-mat/0512058
17. Baxter, R.J.: Proc. R. Soc. Lond. A **383**, 43–54 (1982)
18. Baxter, R.J.: J. Phys. A **19**, 2821 (1986)
19. Baxter, R.J.: J. Phys. A **20**, 5241 (1987)
20. Jacobsen, J.L., Salas, J.: Nucl. Phys. B **783**, 238–296 (2007). cond-mat/0703228
21. Cardy, J.L.: J. Phys. A **17**, L385 (1984)
22. Kostov, I.: J. Stat. Mech. Theory Exp. P08023 (2007). hep-th/0703221
23. Martin, P., Saleur, H.: Lett. Math. Phys. **30**, 189 (1994)
24. Pasquier, V., Saleur, H.: Nucl. Phys. B **330**, 523–556 (1990)
25. Jacobsen, J.L., Salas, J.: J. Stat. Phys. **122**, 705–760 (2006). cond-mat/0407444
26. Chang, S.-C., Shrock, R.: Int. J. Mod. Phys. B **21**, 1755–1773 (2007). cond-mat/0602178
27. Dubail, J., Jacobsen, J.L., Saleur, H.: (to be published)